

Nonlinear Analysis of Punching Behavior of Flat Slab at Corner Column Under Effect of Vertical Load

¹Hala Atef Ahmed, ²Ayman Hussein Hosny Khalil, ³Mahmoud Mohamed El-Kateb

¹M. Sc. Student, Structural Engineering Department, Faculty of Engineering, Ain Shams University, Egypt

²Professor, Structural Engineering Department, Faculty of Engineering, Ain Shams University, Egypt

³Associate Professor, Structural Engineering Department, Faculty of Engineering, Ain Shams University, Egypt

Abstract - In this study, a non-linear 3D numerical analysis using ANSYS was performed to investigate the influence of slab and column dimension on the punching shear capacity of the corner slab-column connection. Most research studied the punching shear stress, but none of them studied the distribution of punching shear stress, which was assumed to be linear in different codes. Verification models have been used to simulate existing experimental data. Two factors were taken into consideration for their influence on the punching shear strength of the concrete: the slab aspect ratio, column aspect ratio, and other factors are constant. Therefore, twenty-one models of different slab and column dimensions were investigated, and a comparison between the results obtained by the finite element analysis and the numerical results was made. Also, a comparison between shear stresses computed using two different methods in the Egyptian code, the simplified method, and the detailed method, and compare them with the Ansys models.

Keywords: Corner slab-column, Nonlinear analysis, Unbalanced moment, punching stress, column size, Egyptian code.

I. INTRODUCTION

Punching shear failure is considered as one of the most critical failure mechanisms in structural members, especially flat slabs. It is a brittle, sudden failure that happens around a column or under an area of concentrated load. This type of failure cannot be easily predicted. A significant portion of the concentrated load is applied to a small area of the loaded concrete slab because of the reaction of a column against it, which causes punching shear. The presence of an unbalanced moment that is passed from the slab to the column may raise the possibility of punching shear failure, and the combination of shear and unbalanced moment is unavoidable, especially in the corner column. Different span lengths, unevenly distributed gravity loads, and any lateral loads lead to increasing the unbalanced moment. Thus, increasing punching shear failure. The flexural reinforcement, the thickness of the slab, the loaded area, shear reinforcement, and the size of the

column all enhance punching shear strength, and it becomes easy to decrease punching shear failure.

Many codes and studies have presented various formulas for calculating punching shear strength. Punching strength is predicted by considering many factors: a control perimeter, an effective depth, the concrete strength as discussed in ACI 318-19 [1] and ECP 203-2020 [2] codes, and also the reinforcement ratio as discussed in Euro code [3].

Both the ACI [1] and ECP [2] codes assumed that the critical section for punching shear is placed at $(d/2)$ in the column's face. A nonlinear analysis was conducted to assess the magnitude and distribution of eccentric shear and flexural moments at the critical section at $d/2$ of the corner edges.

The Egyptian and ACI codes provide a method for calculating punching shear stress due to both gravity and moment transferred to the column. Also, Egyptian code offers an additional simplified method which calculates punching shear stress due to gravity only and multiplies it with a magnification factor β to take into account the transferred moment; however, the results of this method do not agree well with the code-detailed method. In this paper, a modification to the simplified method is proposed. The shear stress in both codes ACI and ECP assumed to vary linearly. But, as this study will demonstrate, the load on the critical section is no longer uniformly distributed.

A numerical analysis using a finite element method has been done to calibrate the behavior of corner column-slab connections, and it demonstrated that the models outperformed the experimental results. Thus, using a finite element method ANSYS was used to investigate some parameters in this study especially the dimensions of slab and column of the corner connections.

1.1 Codes provisions

The ACI 318-19 [1] code and ECP 203-2020 [2] (exact method) assume a critical shear section located at $d/2$ from the loaded area or column faces. In the presence of unbalanced moment (M_u) from a slab to a column, the maximum factored

shear stress q_u at a critical section produced by the combination of factored shear force V_u and unbalanced moments M_{ux} and M_{uy} . a portion of this moment ($\gamma_v M_u$) is transferred by eccentric shear, and the remaining unbalanced moment is transferred by flexure ($\gamma_f M_u$) as illustrated in Eqs 1,2,3 and 4. The shear stress distribution along the critical is assumed to vary linearly about the critical shear section, as shown in Figure 1.

$$q_p = \frac{V_u}{A_c} \beta \quad (8)$$

Depending on the concrete's strength, different codes will typically determine the punching shear strength. Many parameters affect the punching shear capacity, such as slab dimensions and column dimensions.

In the current research phase, experimental work with various parameters is not available. Hence, a corner slab-column connection using nonlinear finite element analysis will be established. First, FE model validation has been created to simulate studies conducted by other researchers.[4],[5]. The validation of the FE model and experiment has shown to be in good agreement. Finally, ANSYS will be used to examine various models with variable column and slab dimensions.

1.2 Finite element modeling

The nonlinear finite element program ANSYS V19.2is used in this study. This program has the ability to illustrate concrete's linear and nonlinear behavior. Concrete is considered an isotropic material until cracking during the linear stage. For the nonlinear part, the concrete may undergo plasticity.

Two validation models are created using the ANSYS V19.2 [6] finite element and comparing numerical simulation results with the experimental tests is presented. One of them for internal slab column connections and the other for external slab column connections. The performance of slab-column connectors was evaluated using finite element analysis.

II. VALIDATION OF FE MODEL BY EXPERIMENTAL DATA

Özgür Anil et al.

The first finite element model verification is a concrete slab tested with dimensions of (2000x2000x120) mm. The objective of this research is to validate the finite element model with the experimental results done by Özgür Anil et al.[4].The compressive strength f_{cu} equals 26 Mpa, and the Poisson ratio is equal to 0.2.Two values of yield stress were considered: $F_y=280$ and $F_y=480$ MPa.

The specimens were supported on all four sides in the vertical direction Y, and only four points at the corner have all translational degrees of freedom and were supported on X, Y and Z to prevent the slab from moving or rotating about its plane, as shown in Figure 2.

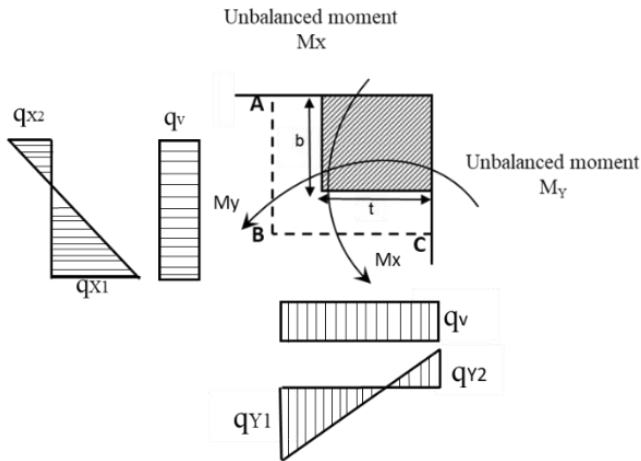


Figure 1: Distribution of shear stress

The nominal shear stress, along perimeters AB and BC, in Figure 1, $v_{u,AB}$ or $v_{u,BC}$, is determined using the following equations:

$$V_{u,AB} = \frac{V_u}{A_c} + \frac{\gamma_v M_{sc} C_{AB}}{J_c} \quad (1)$$

$$V_{u,AB} = \frac{V_u}{A_c} - \frac{\gamma_v M_{sc} C_{AB}}{J_c} \quad (2)$$

$$\gamma_v = 1 - \gamma_f \quad (3)$$

$$\gamma_f = 1 - \frac{1}{1 + \left(\frac{2}{3}\right)\sqrt{\frac{b_1}{b_2}}} \quad (4)$$

The total shear stress at each point for the corner column is computed using Eqs5, 6, and 7.

$$A = q_v - q_{x2} + q_{y1} \quad (5)$$

$$B = q_v + q_{x1} + q_{y1} \quad (6)$$

$$C = q_v + q_{x1} - q_{y2} \quad (7)$$

The Egyptian code offers an alternative, simplified method for calculating the total punching shear stress by assuming a magnification factor β . This factor takes into account the unbalanced moment to calculate the total shear stress q_p as computed in Eq. 8, assuming β factor equal 1.5 for corner column.

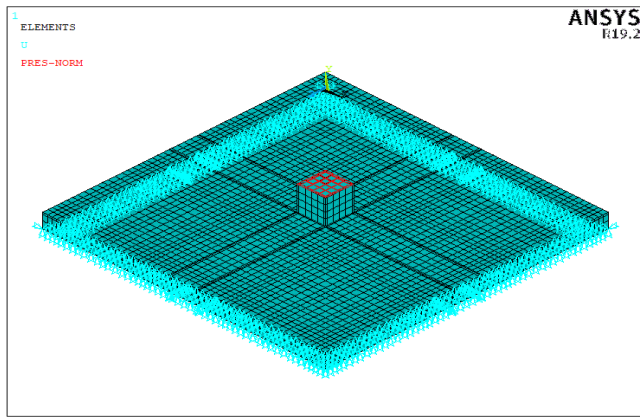


Figure 2: The geometry, boundary conditions and applied loads for slab specimen of Özgür Anil et al

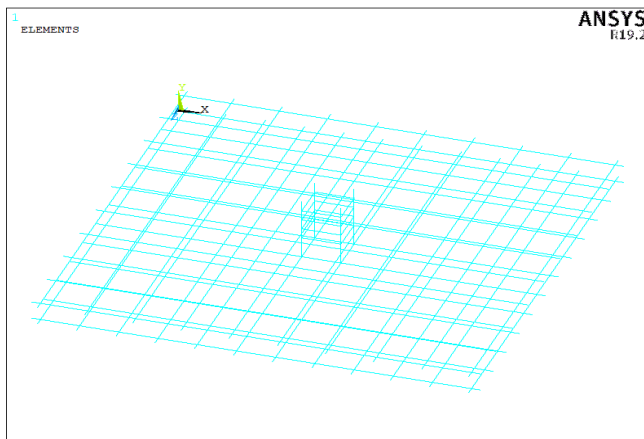


Figure 3: The distribution of reinforcement for slab specimen of Özgür Anil et al

From the model, the maximum punching shear force and the associated maximum vertical deflection are discussed as detailed in Table 1 and Figure 4.

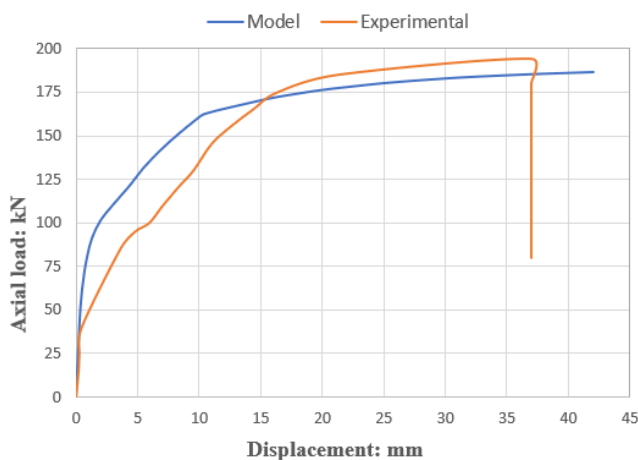


Figure 4: Load–displacement curve of the slab specimen of Özgür Anil et al

Table 1: Comparison between experimental and model results

Control Specimen	Max Applied load (KN)			Max Deflection (mm)		
	V _{Exp}	V _{model}	V _{exp} / V _{model}	δ _{Exp}	δ _{model}	δ _{Exp} / δ _{model}
	193	186	1.038	37.99	37.9	1.002

The load-deflection curves produced from analytical results and the curves obtained from experimental work are in good agreement.

Walker, P. R., and Regan, P. E. 1987

The second finite element model verification is a concrete slab tested by Walker, P. R., and Regan, P. E. 1987[5] with dimensions of (3050x3050x125) mm and column (300x300) mm. The geometry and reinforcement of a quarter of the sample will be created and consist of three specimens with different concrete materials.

Material properties of concrete

Young' modulus ($E_c = 4700\sqrt{f_c}$ MPa) and tensile strength ($f_t = 0.33\sqrt{f_c}$ in MPa), Poisson's ratio for concrete is 0.15. In this study, f_c' for specimens SC1, SC2, and SC3 equal 43.3, 47.9 and 37.4 respectively.

Material properties of steel

The elasticity modulus E_s is taken to be $2E+05$ MPa, Poisson's ratio is assumed to be 0.3, and the yield stress F_y equal to 450 MPa. The control model volumes and mesh geometry for full specimens and quarter part are shown in Figure 5.

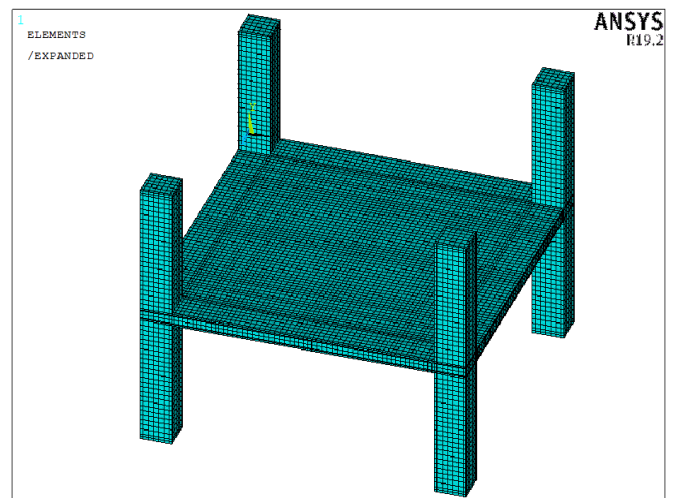


Figure 5: The meshed geometry of the slab specimen

The specimens were supported on four columns, each supported at its all four edge sides in the vertical direction Y,

and only four points at each corner has all translational degrees of freedom and were supported on X, Y, and Z to prevent the slab from moving or rotating about its plane. A quarter an expansion was created then used the symmetry option to produce the full model.

The load is applied incrementally by a force on the loaded points at the top surface of the column, and the slab was loaded on twelve points, three of them at each quarter as shown in Figure 6.

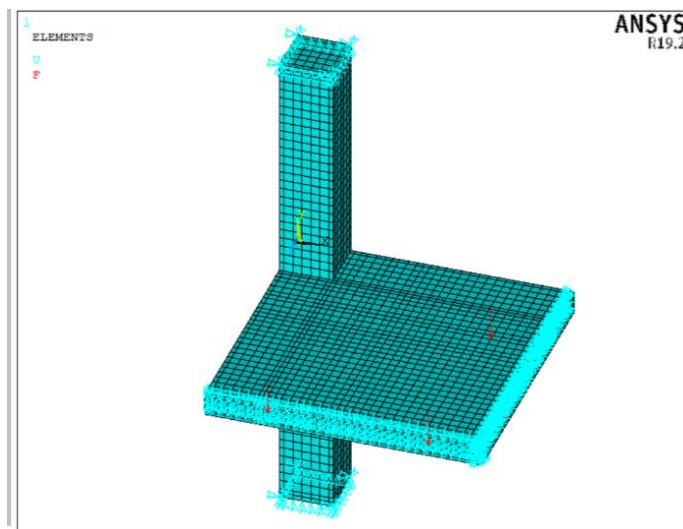


Figure 6: The Boundary conditions and applied loads of the quarter slab specimen

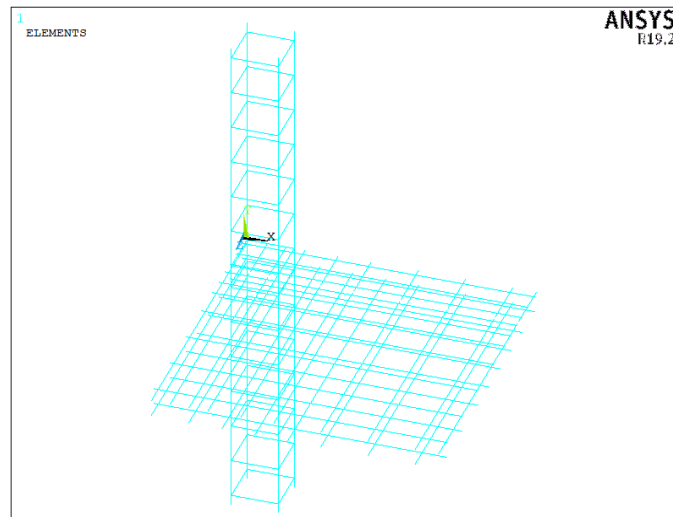


Figure 7: The layout of reinforcement of the control slab specimen (Sectional elevation view)

A comparison between modeling and experiment is stated in Table 2 and Figure 8.

Table 2: Comparison between experimental and model results

Specimens	Ultimate Load (kN)		Max Deflection	P analytical
	Experimental	Analytical	Analytical	P Experimental
SC.1	320	311.8	22.26	0.994
SC.2	297	289.6	19.14	0.975
SC.3	284	291.8	26.91	1.027

Based on these analysis results, it can be concluded that the failure mechanism obtained shows the slabs fail near the columns. The slabs' possible failure appears to be caused by punching. Figure 8 shows the relation between axial load versus average displacement for all specimens (Sc1, Sc2, Sc3).

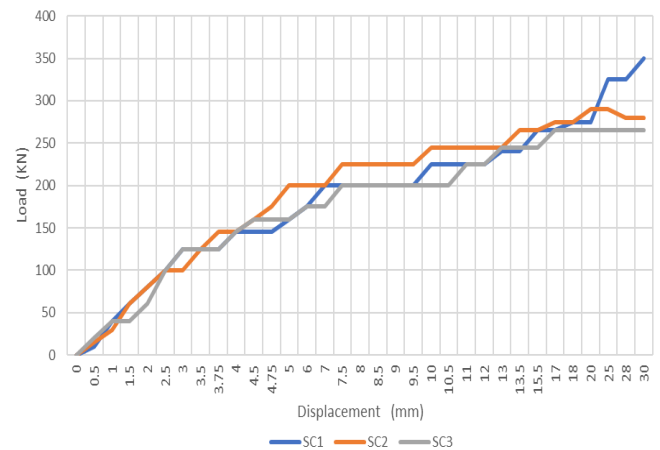


Figure 8: Load–displacement curve of all specimens

The load-deflection curves obtained from analytical results and the curves obtained from experimental work are in good agreement.

The validity of the FE model was established by the conclusion drawn from the two validation models that there was good agreement between numerical FE simulation and the experiment. Furthermore, a detailed overview of geometry, meshing, material, failure criteria, boundary conditions, and non-linear solutions are also covered in the next chapter with different parameters by using ANSYS 19.2.

III. PARAMETRIC STUDY

Non-linear finite-element analysis (ANSYS) will be used to investigate the shear stress at the corner column. A total of twenty-one quarter scale slab-column specimens are modeled due to the symmetry in geometry, loading and supports. Several parameters shall be taken into consideration, such as

- Different aspect ratios of slabs
- Different aspect ratios of columns

Twenty-one specimens of slab-column connections in quarter-scaled finite element models were created. Specimens are divided into three major groups according to slab dimensions and column dimensions; groups **A**, **B** and **C** are divided according to slab dimensions and slab thickness, then each group is divided into sub-sets according to column dimensions. Slabs are reinforced with different flexural reinforcement ratios (1.0%, 1.13% and 1.15%) and with compression longitudinal steel bars with a diameter of 12 mm spaced 125 mm in both directions for all specimens. Columns are reinforced with minimum longitudinal steel bars with a diameter of 22 mm and are confined with transverse stirrups of diameter 10 mm with spacing 200 mm. The columns were modeled with different aspect ratios. Each group deals with seven different columns as a subset for each group, with many aspect ratios (1:1, 3:2, 2:3, 2:1, 1:2, 5:2, 2:5). In Group A, the specimens are modeled with slab dimensions of (3000x3000x140) mm, while subsets in Group B are modeled with slab dimensions of (3000x4000x160) mm, and In Group C the slab dimensions of (3000x5000x180). The analysis modeled the full column height of 1.25 m above and below the slab. The columns were fully fixed at each end. Details of the specimens are shown in Figures 9 and 10.

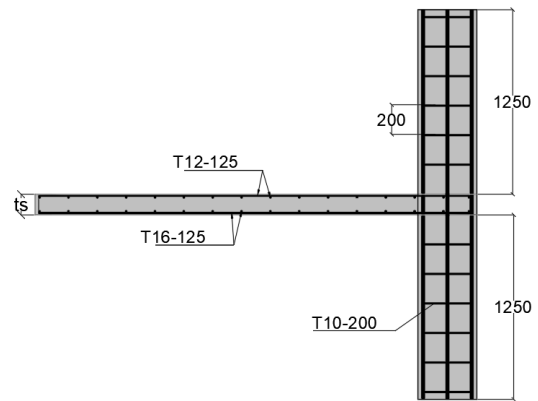
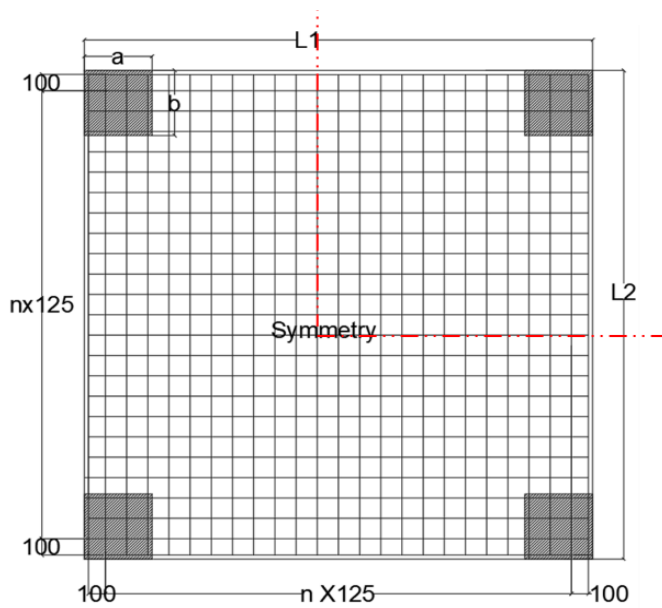


Figure 10: Typical detail of the slab-column specimen

The different dimensions of the column used in the modeling as stated in Figure 11, C1 (400 x 400), C2 (400 x 600), C3 (600 x 400), C4 (400 x 800), C5 (800 x 400), C6 (300 x 750), C7 (750 x 300).



- n : Numbers of spacing
- L1 & L2 : Spans of the slab
- ts : Slab thickness
- a & b : Columns dimensions
- * All dim in mm .

Figure 9: Finite Element model layout

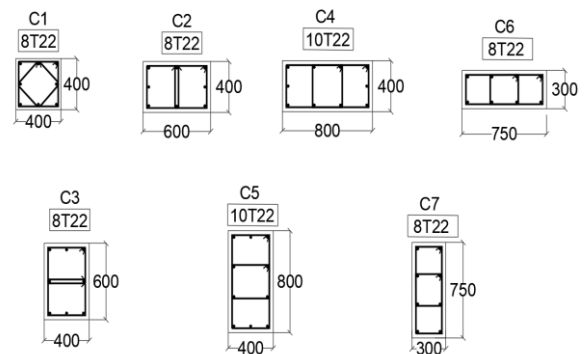


Figure 11: Details of columns' dimensions and reinforcement of all specimens

Compressive concrete strength (f_{cu}) used for all test specimens is equal to 30 MPa, Yield strength= 350 Mpa, Open and close shear transfer coefficient=0.2 and 0.8 respectively.

Loading and Boundary condition

Displacement boundary conditions are used to constrain the model. The column is constrained in the Y-direction, and four-quadrant nodes are constrained in both directions, x and z to prevent rotation. For Symmetry boundary condition, area support for slab edges had been assigned to all free slab edges, as shown in Figure 12.

Loading to finite element model is done using loading steps concept applying gravity loads gradually for solution convergence. Loads were distributed uniformly and increased proportionately until failure.

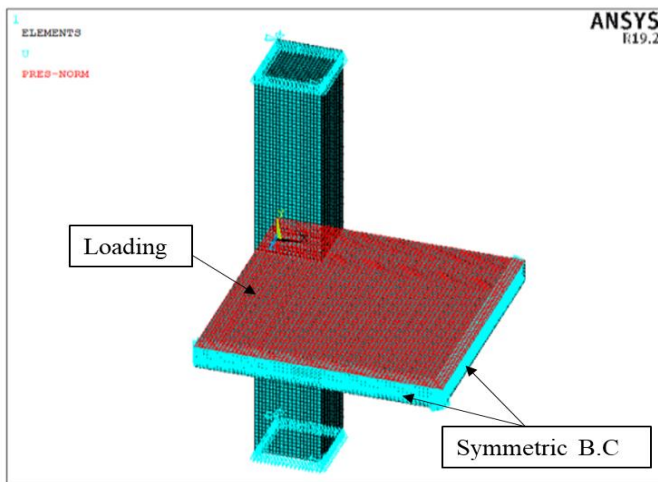


Figure 12: Supports boundary condition and the uniform load of all specimens

III. RESULTS AND DISCUSSIONS

The results of the FE analysis of each model obtained from this study show that the ultimate punching shear load is described in terms of load at failure and the corresponding slab deflection. The results of the finite element models are summarized in Table 3.

Table 3: Load carrying capacity for all specimens

Group ID	Spec	Slab Dim		Column		Ansys Result	
		Dims (mm)		ID	Dims (C1 X C2)	Vult (KN/m2)	σ_{ult}
A	S01	3000 x 3000 x 140		C1	400 x 400	30	9.0
	S02			C2	400 x 600	28.09	4.7
	S02*			C3	600 x 400	27.98	4.5
	S03			C4	400 x 800	32.42	2.9
	S03*			C5	800 x 400	32.42	2.4
	S04			C6	300 x 750	30.21	5.0
	S04*			C7	750 x 300	31.32	4.8
B	S05	3000 x 4000 x 160		C1	400X400	25.52	11.3
	S06			C2	400 x 600	21.82	5.4
	S06*			C3	600 x 400	23.48	5.5
	S07			C4	400 x 800	32.65	9.0
	S07*			C5	800x400	31.15	4.5
	S08			C6	300 x 750	23.48	4.9
	S08*			C7	750 x 300	27.65	4.9
	C			S09	3000 x 5000 x 180		C1
S10		C2	400 x 600	25.45			25.0
S10*		C3	600 x 400	20.35			7.8
S11		C4	400 x 800	17.89			21.2
S11*		C5	800 x 400	14.79			2.0
S12		C6	300 x 750	16.85			7.2
S12*		C7	750 x 300	16.02			4.3

The relation between load and deflection for all 21 specimens is illustrated in Figure 13.

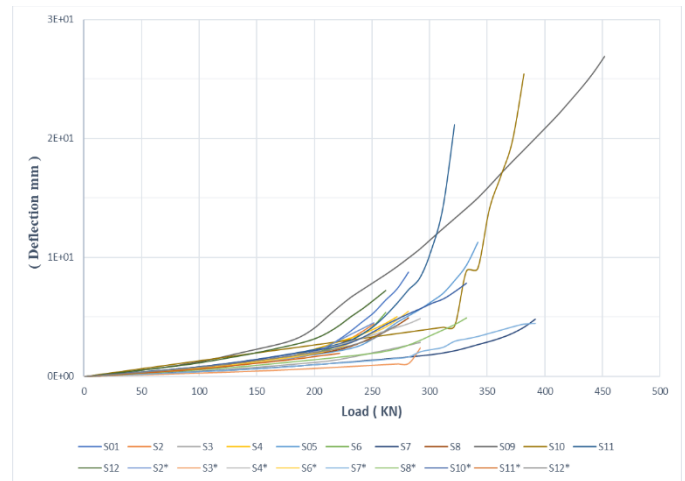


Figure 13: Load–deflection relation of all specimens

Shear stress at paths around $d/2$ from the column face represents the shear stress at XZ extracted from Ansys as shown in Figure 14 to get the shear stress on the critical section, which is no longer uniformly distributed, and compare results with the shear stress calculated using codes.

Figure 14 shows the shear stress for specimen S01 at points A, B and C. The shear stress for other specimens was extracted from the model in the same way, and the results are illustrated in Table 4.

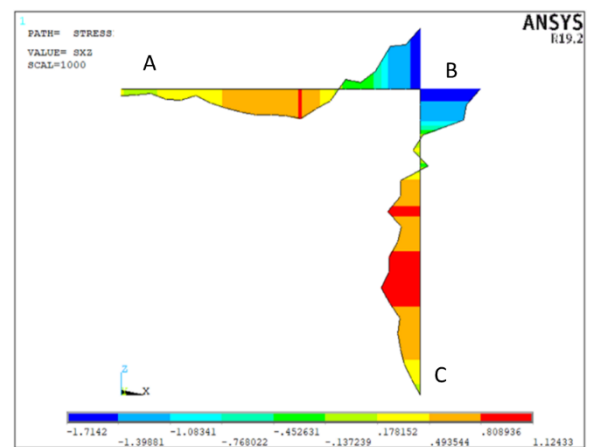


Figure 14: Shear stress at a critical section for S01

A non-linear finite-element analysis was determined to calculate the punching shear stresses using the detailed method according to the Egyptian code. The punching shear stresses due to gravity load only are calculated. The magnification factor β to account for the additional shear stress due to moments transferred to columns is the ratio between the calculated total punching shear stress using the detailed method using unbalanced moment and the punching shear stress due to gravity loads. A comparison between the shear stress from the model and the code ECP is illustrated in Table 4.

Table 4: Comparison between the shear stress from the model and the shear stress from both codes ECP 203-2020 and ACI code and values of β

Group	Spec	Ansys result		ECP- code		ACI- code		β
		q_{max} (N/mm ²)	q_v (N/mm ²)	q_{cup} (N/mm ²)	q_{max}/q_{cup}	q_c (N/mm ²)	q_{max}/q_c	
A	S01	1.72	0.91	1.413	1.22	1.21	1.42	1.89
	S02	1.21	0.67	1.413	0.86	1.21	1.00	1.80
	S02*	1.25	0.67	1.413	0.88	1.21	1.03	1.86
	S03	1.02	0.62	1.341	0.76	1.14	0.89	1.65
	S03*	1.08	0.62	1.341	0.81	1.14	0.94	1.74
	S04	1.31	0.69	1.272	1.03	1.09	1.20	1.91
	S04*	1.3	0.69	1.272	1.02	1.09	1.19	1.90
	S05	1.89	0.91	1.413	1.34	1.21	1.55	2.06
B	S06	1.22	0.64	1.413	0.86	1.21	1.01	1.91
	S06*	1.34	0.68	1.413	0.95	1.21	1.11	1.98
	S07	1.31	0.74	1.413	0.93	1.21	1.08	1.76
	S07*	1.37	0.71	1.413	0.97	1.21	1.13	1.92
	S08	1.33	0.65	1.272	1.05	1.09	1.21	2.03
	S08*	1.54	0.75	1.272	1.21	1.09	1.41	2.06
	S09	2.3	1.15	1.413	1.63	1.21	1.90	1.99
	S10	1.7	0.81	1.413	1.2	1.21	1.40	2.11
C	S10*	1.53	0.67	1.413	1.08	1.21	1.26	2.29
	S11	1.06	0.5	1.413	0.75	1.21	0.87	2.11
	S11*	0.81	0.44	1.413	0.57	1.21	0.67	1.87
	S12	1	0.55	1.272	0.79	1.09	0.92	1.81
	S12*	1.28	0.53	1.272	1.01	1.09	1.17	2.41

Table 4 shows that the values of the shear stress calculated from the model and the shear stress calculated from the code are in good agreement.

From the table, it is obvious that the value of β . Thus, a value of β for a corner column is about 50% more than the current code value, and it is observed that the dimension of the column and the rotation have a significant effect on the punching stress and the value of β as shown in Figure 15 and 17.

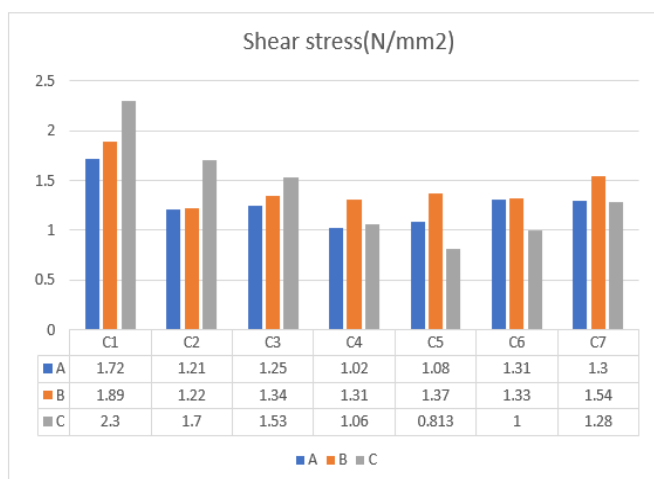


Figure 15: The relation between max shear stress and different spans with different columns dimensions

A For slab (3000x3000x140) and **B** for (3000x4000x160) and **C** for (3000x5000x180).

As per ECP-203-2020, the β for the corner columns is equal to 1.50, which is a low value to be used for a simplified method, as shown in Figure 16.

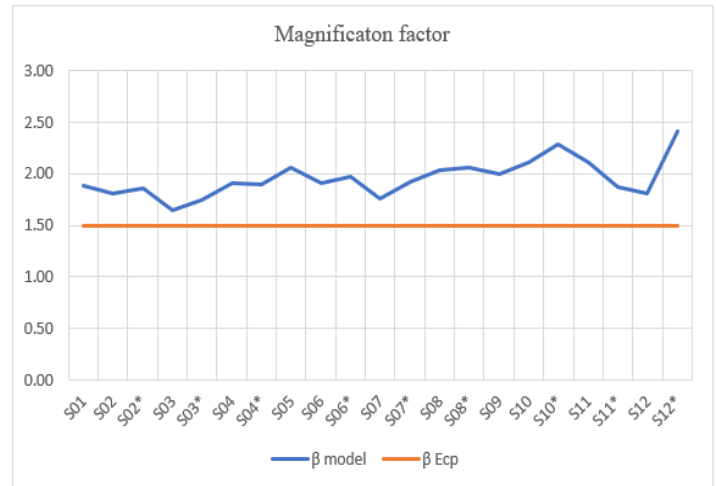


Figure 16: Comparison between values of β from the simplified method and from the detailed method in ECP code for corner column

The method implies that the estimated additional increase in shear stresses due to the moment transferred from slab to column is about 50% for the corner column. Furthermore, a discrepancy between the two methods because the punching shear stresses resulting from moment transfer using the detailed method depend on several variables, including the slab dimension, the thickness of the slab, and the size of the columns, which were not considered in the simplified method.

It is observed that the analytical results obtained from ANSYS 19.2 [6] are in good agreement with the ECP 203-2020 [2] predictions as the ratio q_{max}/q_{ECP} are around one.



Figure 17: The relation between β value and different spans with different columns dimensions

IV. CONCLUSION

Based on the analytical study using ANSYS 19.2[6] software, the following conclusions can be summarized:

- The non-linear analytical results were in good agreement with the experimental results of the ultimate punching load and the max shear stress.
- The shear stress due to moment transfer changes considerably by many factors, such as slab and column dimensions.
- The shear stress on this critical section is distributed non-uniform, which contradicts the ECP 203-2020 and ACI 318-19 codes, which assume the stress varies linearly.
- Increasing the slab dimensions leads to an increase in the transferred moment and the shear stress, which consequently increases the β factor.
- The β factor for the corner column in ECP 203-2020 is equal to 1.5, but from the model result, the slab dims. (3000x3000), the β factor increased ranging from 20 to 26%, and an increased about 30 to 38% for slab dims. (3000x4000) and about 50% to 60% for slab dims. (3000x5000), As discussed in research [7].
- An increase in the column dimensions leads to a decrease in the shear stress clearly because the shear stress due to vertical load decreases as the critical section increases and, accordingly, the total shear stress decreases.
- For column (400x800), the shear stress is less value compared to other columns' dimensions for the slab with dimension (3000x3000) and the $\beta = 1.65$, which is close to the value from the code $\beta = 1.5$ and for the slab dim (3000x4000), the $\beta = 1.76$ and $\beta = 2.1$ for slab dim (3000x5000).
- From the previous conclusion, it was noticed that increasing the column dimension and decreasing the slab dimensions lead to a decrease in the value of shear stress and the β value.
- A new value of β recommended by multiplying the β with a factor that depends on the column and slab dimensions.

V. RECOMMENDATION

Depending on the outcomes of this study, more parameters need to be investigated to accurately predict the real punching shear stress of the slab corner column connections, such as a greater number of column aspect ratios, different slab aspect ratios, and different depths.

The β value in the ECP code should be increased according to the slab and column dim, which may vary from 2 to 2.5, and use these modified values instead. Otherwise, it is suggested to ignore the simplified method for the corner column and use the exact method.

REFERENCES

- [1] "ACI 318-19 Building Code Requirements for Structural Concrete (ACI," 2019.
- [2] E. C. P. 203-2020, "Egyptian code for design and construction of reinforced concrete, 2020.
- [3] Design of concrete structures- part1-1 General Rules and Rules foe Buildings " Eurocode 2,British, London: Standards Institution , 2004.
- [4] Anil, Kina and Salmani, "Effect of opening size and location on punching shear behaviour of two-way RC slabs," *ICE Publishing*, vol. 66 Issue 18, p. 955–966, 2014.
- [5] P. R. Walker and P. E. Regan, "Corner column-slab connections in concrete flat," *Journal of Structural Engineering*, , Vols. 113(4),, pp. 704-720, 1987.
- [6] "ANSYS Help. 19.2 Manual," in ANSYS, 2019.
- [7] M. T. ELMIHILMY1, "Modification to the simplified method for calculation punching shear stresses for flat slab system in the EC-2001," *Journal of engineering and applied science* , Vols. 48, NO. 5, pp. 883-900, OCT. 2001.

Citation of this Article:

Siddhant Nigam, Hariom Pareek, Avinash Vishwakarma, Ritik Pareek, Dr. Roopali Lolage, "Nonlinear Analysis of Punching Behavior of Flat Slab at Corner Column Under Effect of Vertical Load" Published in *International Research Journal of Innovations in Engineering and Technology - IRJIET*, Volume 7, Issue 4, pp 119-126, April 2023. Article DOI <https://doi.org/10.47001/IRJIET/2023.704019>
